ELSEVIER

European Journal of Pharmaceutics and Biopharmaceutics 53 (2002) 75–86

European Journal of Pharmaceutics and Biopharmaceutics

www.elsevier.com/locate/ejphabio

Research paper

Crystal forms of torasemide: new insights ☆

Judith Maria Rollinger*, Elisabeth Maria Gstrein, Artur Burger

Institute of Pharmacy/Pharmacognosy, University of Innsbruck, Innsbruck, Austria

Received 2 February 2001; accepted in revised form 17 August 2001

Abstract

Crystallization from various organic solvents results in three crystal forms of torasemide: monotropically related mod. I (melting point, 158–161°C) and mod. II (melting point, 155–158°C), as well as a pseudopolymorphic crystal form (form A, channel inclusion compound with 1.9–4.2% water and alcohol). Physicochemical properties were determined by thermoanalysis (hot-stage microscopy, differential scanning calorimetry, thermogravimetry), Fourier transform infra-red and Raman spectroscopy, and X-ray powder diffractometry. The hygroscopicity, relative stability, true density, and heat of solutions were determined, respectively. The dissolution behaviour of mod. I and II was investigated as a function of pH, temperature, and in addition to surfactants. Mod. II is nearly three times more soluble than mod. I (mod. I, 0.34 mmol l^{-1}; mod. II, 0.93 mmol l^{-1} at 20°C, pH 4.90) and proved to be highly kinetically stable. By crystallization from 1-butanol, a new compound was synthesized, which was identified as [[4-[(3-Methylphenyl)amino]-3-pyridinyl]sulfonyl]-carbamic acid, butyl ester (TOBC). The most important properties of this torasemide derivative are given. The present results give a thorough physicochemical characterization of the crystal forms of torasemide. They clearly indicate a mistaken identity of mod. II with crystal form A in formerly published articles.

Keywords: Torasemide; Polymorphism; Monotropism; Channel inclusion compound; Thermal analysis; Fourier transform infra-red spectroscopy; Raman spectroscopy; X-ray powder diffractometry; Solubility; [[4-[(3-Methylphenyl)amino]-3-pyridinyl]sulfonyl]-carbamic acid, butyl ester

1. Introduction

Torasemide, *N*-[[(1-Methylethyl)amino]carbonyl]-4-[(3′-methylphenyl)amino]-3-pyridinesulfonamide, is a lipophilic anilinopyridine sulphonylurea derivative (1) with pharmacological properties of a high ceiling loop diuretic. Its nearly complete bioavailability over a broad dose range from 2.5 up to 200 mg matches the requirements for the treatment of both acute and chronic congestive heart failure and hypertension [2,3]. It is used as drug substance, for example in Demadex®, Toradiur®, Torem®, and Unat®.

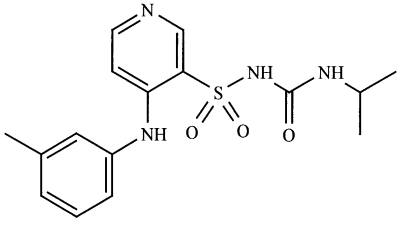

In 1978, Dupont et al. [4,5] described the crystal structures of two different crystal forms of torasemide: form I was stated to crystallize monoclinic $P2_1/c$ with a melting point of 169°C, whereas the crystal structure of form II was identified as monoclinic P2/n with a melting point of 162°C. In the European Patent of F. Topfmeier and G. Lettenbauer of 1986 [6], the problematic simultaneous crystallization of two modifications of torasemide is discussed. These modifications are assigned to the crystal structures of Dupont's form I and II due to their melting points being comparable with Dupont's forms. A process for the preparation of crystalline torasemide in pure mod. I from torasemide of mod. II is claimed. In the United States Patent of 1994 [7], the same inventors correct the melting points of both modifications to distinctly lower temperatures of 159–161.5°C for mod. I and 157.5–160°C for mod. II. On investigation of the physicochemical properties of torasemide (mod. I), Kondo et al. also mentioned a second modification [8]. They referred to the published crystal structures of Dupont et al. and depicted IR spectra and powder X-ray diffraction patterns of mod. I and II in their article. In the recently published work of Danilovski et al. [9], a novel, and therefore, third crystal structure, denoted as T-N, is fully described.

The aim of this study was to fully characterize all of the crystal forms obtained by crystallization from different

☆ Part of this work was presented at the 14th Wissenschaflichen Tagung der Österreichischen Pharmazeutischen Gesellschaft in Graz, Austria, June 11–13, 1998 [1].

* Corresponding author. Institute of Pharmacy/Pharmacognosy, University of Innsbruck, Innrain 52, Josef-Moeller-Haus, A-6020 Innsbruck, Austria. Tel.: +43-512-507-5308; fax: +43-512-507-2939.

E-mail address: judith.rollinger@uibk.ac.at (J.M. Rollinger).

0939-6411/02/$ - see front matter
PII: S0939-6411(01)00206-5

solvents, to assign them to reported crystal structures, and to find a plausible explanation for the melting point discrepancies given in literature. A detailed physicochemical and thermodynamic characterization of all crystal forms of torasemide is aspired to enlighten the analytical aspects and to ensure the application of the optimal crystal form in regard to stability, technological properties, and economical reasons.

2. Materials and methods

The studies were carried out with torasemide mod. I (batch number, EK 64/166) and mod. II (batch number, 445 463-01), particle size 30–70 μm, respectively, obtained from Roche Diagnostics GmbH (Mannheim, Germany). All solvents and chemicals used for this study were of analytical grade.

2.1. Thermoanalysis

Hot-stage microscopy was performed using a Reichert–Thermovar polarizing microscope fitted with a Kofler hot-stage (Reichert, Vienna, Austria).

Differential scanning calorimetry (DSC) was carried out with a DSC-7 (Perkin–Elmer, Norwalk, CT) using the Pyris Software version 2.0 for Windows. The sample masses for quantitative analysis were 1–3 ± 0.0005 mg (Ultramicroscales UM3, Mettler, Greifensee, Switzerland), weighed into perforated aluminium sample pans (25 μl). Nitrogen 5.0 (20 ml min^{-1}) was used as purge gas. The temperature axis was calibrated with benzophenone (melting point, 48.0°C) and caffeine (melting point, 236.2°C). Enthalpy calibration of the DSC signal was performed with indium 99.999% (Perkin–Elmer, Norwalk, CT). The applied heating rate (HR) was 5 K min^{-1}. Stated temperature values from DSC measurements are extrapolated onset temperatures.

Thermogravimetry (TG) was carried out with a TGA-7 instrument (Perkin–Elmer, Norwalk, CT); 50-μl platinum sample pans were used and purged with nitrogen 5.0 (balance purge, 40 ml min^{-1}; sample purge, 20 ml min^{-1}). The sample weight was about 1–5 ± 0.0005 mg and the HR was 5 K min^{-1}. Mass calibration was performed with a 100.0-mg calibration weight (Perkin–Elmer), temperature calibration was carried out with alumel (magnetic transition temperature, 163.0°C) and nickel (magnetic transition temperature, 354.0°C).

2.2. X-ray powder diffraction

X-ray powder diffraction patterns were obtained with a Siemens D-5000 X-ray diffractometer (Siemens AG, Karlsruhe, Germany) equipped with θ/θ-goniometer (tube voltage, 40 kV; tube current, 40 mA), applying a scan rate of 0.005° 2θ s^{-1} in the angular range of 2–40° 2θ. The single crystal data [4,5,9] were used to calculate the idealized X-ray powder pattern for a Cu K_α radiation with the program *PowderCell for Windows* [10].

2.3. Fourier transform infra-red-spectra

Fourier transform infra-red (FTIR)-spectra were recorded with a Bruker IFS 25 FTIR-spectrometer (Bruker Analytische Meßtechnik GmbH, Karlsruhe, Germany) connected with a Bruker FTIR-microscope (15× Cassegrain-objective and visible polarization). Samples were scanned as potassium bromide pellets (diameter, 13 mm; 1 mg torasemide to 270 mg potassium bromide; pressure, 740 MPa) at an instrument resolution of 2 cm^{-1} in the spectral range from 4000 to 600 cm^{-1} (50 interferograms/spectrum). For FTIR-microscopy, small samples were rolled on a zinc selenide window (13 × 2 mm) and recorded at an instrument resolution of 4 cm^{-1} (focus diameter, 50 μm; 100 interferograms/spectrum).

2.4. FT-Raman spectra

FT-Raman spectra were recorded with a Bruker RFS 100 FT-Raman spectrometer (Bruker Analytische Meßtechnik GmbH, Karlsruhe, Germany) equipped with a diode-pumped Nd:YAG laser (1064 nm) as the excitation source and a liquid nitrogen-cooled high-sensitivity detector. The powder samples were packed into small aluminium cups, and the spectra were recorded at an output power of 200 mW (64 scans at 4 cm^{-1} instrument resolution).

2.5. Density measurements

The specific volume of the crystal forms was determined by an air comparison pycnometer (Ultrapycnometer 1000, Quantachrome Corp., Syosset, NY). The samples (approximately 1 g) were purged with helium for 15 min, and calibration was carried out with a steel-sphere ($V = 1.0725$ cm^{-3}). The mean of three parallel determinations was taken, at least of two different sample weights of the sample.

2.6. Solution calorimetry

The solution calorimetric experiments were performed in methanol at 40.0°C with an isothermal precision calorimetry system (LKB 8700-1, LKB-Produkter AB, Bromma, Sweden) equipped with a precision thermostatic water bath, LKB 7600, and a 100-ml glass reaction vessel. The electrical calibration system was checked by chemical calibration with the enthalpy of reaction of TRIS (Tris(hydroxymethyl)aminomethane p.a., Merck, Darmstadt, Germany) in 0.1 mol l^{-1} HCl at 25°C (N.B.S.-724a: −29765 ± 10 J mol^{-1}). The used sample mass was about 100 ± 0.1 mg. Temperature change was calculated by graphical extrapolation based on Dickinson's method [11]. Measurements were performed in triplicate.

2.7. Sorption kinetics

The determination of moisture uptake was studied gravimetrically at 25°C and 92% relative humidity (RH), using special hygrostates [12] and a below-weighing Mettler semi-micro balance AT 261 (Mettler Instruments AG, Greifensee, Switzerland). The ground sample mass was about 250–300 mg each (±0.02 mg). The RH in the semi-micro-hygrostates was adjusted with phosphorus(V)oxide (RH, 0%) and a saturated aqueous solution of potassium nitrate (RH, 92%).

2.8. Solubility behaviour

The concentration of dissolved samples (from stirred suspensions at constant temperatures, ±0.1 K, as described in [12]) was determined spectrophotometrically with a Shimadzu UV spectrophotometer 160 A (Shimadzu Corp., Kyoto, Japan). Solubility measurements dependent on temperature were carried out in 1-butanol at 4.0, 12.0, 20.0, 29.0, 38.0 and 47.0°C. Withdrawn samples were diluted with 1-butanol and measured at 286.0 nm ($\varepsilon = 11,552$ mol^{-1} cm^{-1}) against 1-butanol as a blank. Solubility measurements dependent on pH-buffer solutions of pH 1–pH 8 were prepared in accordance with Sörensen. After stirring the suspensions for about 30 min at each pH-value, at least three samples were withdrawn and diluted with the standard buffer solution of pH 6.881 (20°C). The samples were measured at 286.0 nm ($\varepsilon = 12,500$ mol^{-1} cm^{-1}) against the standard buffer solution of pH 6.881 as a blank. Solubility measurements dependent on detergent addition were determined at 20.0°C in Na_2HPO_4/KaH_2PO_4-buffer solution (pH 4.966) with the addition of 0.0025, 0.005, 0.010, 0.015, 0.030, 0.060 and 0.090% of polysorbate 80, respectively. After 2 h, the samples were measured as described above (solubility measurements depending on pH).

2.9. Coulometry

The water content of crystals was determined by a Mettler KF-Coulometer DL 37 (Mettler-Toledo AG, Darmstadt, Germany) using pyridine-free reagents (Merck, D-Darmstadt, Germany). Measurements were performed in triplicate.

2.10. Determination of ethanol

The ethanol content of crystals was determined by enzymatic analysis (ADH-method). The solvent used was a diphosphate buffer solution (pH 9.0).

3. Results

3.1. Preparation of crystal forms

From crystallization experiments, three different crystal forms of torasemide were identified (mod. I, mod. II, form A), as well as a new compound, designated as TOBC. This, so far unknown, substance was analyzed by mass spectrometry and ^{1}H-NMR spectroscopy (data available on request from the authors) as [[4-[(3-Methylphenyl)amino]-3-pyridinyl]sulfonyl]-carbamic acid, butyl ester , $C_{17}H_{22}N_3O_4S$ (M_r, 363.4).

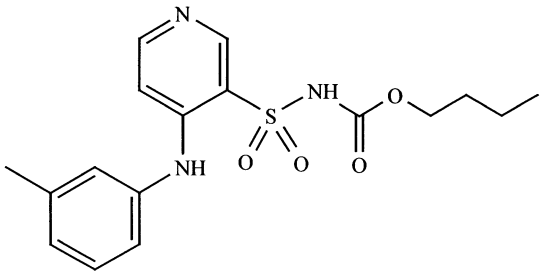

It was obtained by dissolving torasemide in 1-butanol and heating up the solution to boiling point for about 3 min. From this solution, crystals were formed at ambient temperature within 1 day. TOBC continuously decomposes during the melting process, which lies between 157 and 169°C. FTIR- and Raman spectra are shown in Fig. 1.

Torasemide mod. I crystallizes from a hot saturated solution of methanol, ethanol (96%), ethanol absolute, 1- or 2-propanol by slowly cooling down to 20°C. Mod. II can quantitatively be obtained by precipitation of a sodium hydroxide solution ($c = 1$ mol l^{-1}) with an equimolar acetic acid solution at 20°C. Torasemide crystal form A is prepared by rapidly cooling down a hot saturated solution of ethanol 96%/water or methanol/water (v/v = 2:1, respectively) to 7°C. After about 24 h, crystals were filtered off, and stored at ambient conditions. Form A does not crystallize from pure alcohol or water. However, small amounts of water in solvents, i.e. in ethanol, 1- or 2-propanol, are sufficient to let a few crystals of form A crystallize, if the hot solution is rapidly cooled down to 7°C.

3.2. Identification and characterization of the crystal forms

The most relevant results and data of the three crystal forms of torasemide are given in Table 1. Mod. I crystallizes in the form of colourless prisms or needles. By hot-stage microscopy, the melting process of these crystals lies between 158 and 161°C and is followed by thermal decomposition indicated by the formation of small bubbles in the melt, which turns slightly brownish at these temperatures. Mod. II consists of colourless micro-crystalline aggregates. Its melting process lies 3 K lower than that of mod. I, but shows an analogous melting and decomposition behaviour.

Crystal form A consists of transparent, rhombic or hexagonal platelets up to 5 mm dimension (Fig. 2a). In preparation with silicone oil, transformation of these crystals is detectable by hot-stage microscopy, perceptible by a distinct formation of bubbles and loss of transparency of

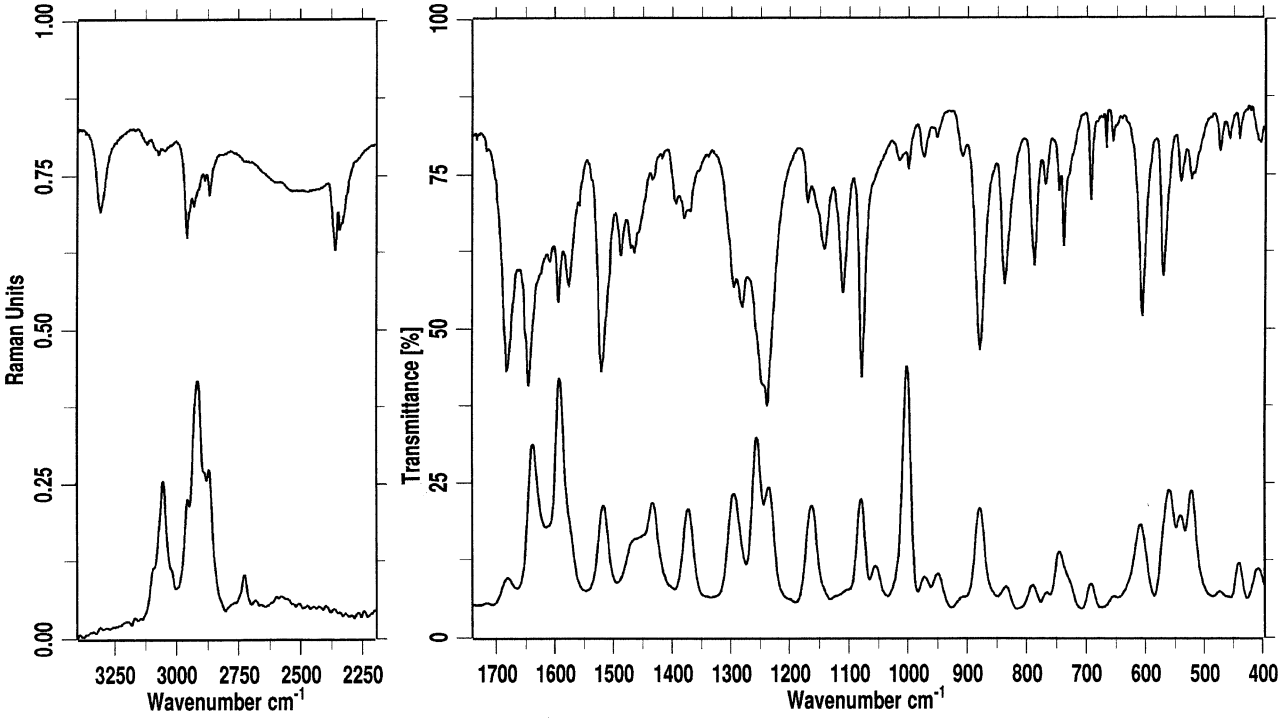

Fig. 1. FTIR- and Raman spectrum of [[4-[(3-Methylphenyl)amino]-3-pyridinyl]sulfonyl]-carbamic acid, butyl ester (TOBC).

Table 1
Characteristic physicochemical properties of torasemide crystal forms

Crystal form	Mod. I	Mod. II	Form A
Habit	Prisms, needles	Micro-crystalline aggregates	Rhombic platelets
Melting point (°C)			–
Hot-stage microscopy	158–161	155–158	
DSC	161.5[a]	157.0[a]	
Enthalpy of fusion (kJ mol^{-1}) ±95% CI	37.2 ± 1.9[a]	29.0 ± 0.9[a]	–
Enthalpy of transition (kJ mol^{-1})[a] ±95% CI	–	~−8.2[b]/−4.4[c]	9.8–14.0[d]
Transition into mod.	–	I	II
At temperature (°C)	–	~160[b]/~40[c]	110–130
Enthalpy of solution (kJ mol^{-1}) ±95% CI[e]	38.89 ± 1.04	34.51 ± 0.67	35.10 ± 0.33
Solubility (mmol l^{-1}) at 20°C, pH 4.90	0.34	0.93	–
True density (g cm^{-3}) ±95% CI[f]	1.363 ± 0.001	1.302 ± 0.009	1.285 ± 0.005
Characteristic IR bands (cm^{-1})	3353	3356	–
	3280	3327	3329
	2978	2965	2972
	1697	1704[g]	1704[g]
	1634	1638	1643
	1611	1618	1608
	–	1559	1556
	1302	1276	1278
	1047	1041	1047
	775	765	762

[a] HR, 5 K min^{-1}, perforated pan.
[b] Virtual: calculated by the difference of enthalpies of fusion.
[c] Virtual: calculated by the difference of enthalpies of solution.
[d] Enthalpy of transition including enthalpy of desolvation, values strongly fluctuating caused by varying content of solvent.
[e] In methanol, 40.0°C.
[f] Measured by pycnometry.
[g] Weak absorption band.

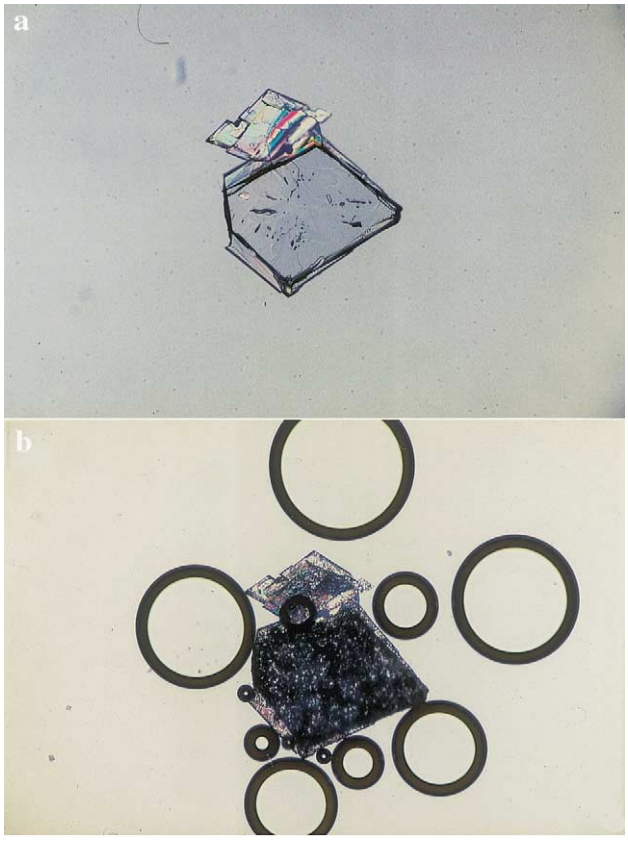

Fig. 2. Micrograph of crystal form A in silicon oil: (a), at room temperature (1 cm ≈ 100 μm); (b), at 125°C (1 cm ≈ 100 μm).

the crystals between 110 and 130°C (Fig. 2a,b). The resulting crystal form was identified as mod. II by FTIR-microscopy. The melting point of form A could not be detected.

DSC-curves of mod. I and II show very similar endotherms of their melting process (Fig. 3). However, their enthalpies of fusion differ considerably (about 28%; Table 1), indicating a large energetic difference concerning the position of H-isobars of mod. I and II at melting temperatures. In the DSC-curve of crystal form A, the endothermic peak between 105 and 130°C (Fig. 3) represents a desolvation, which is obviously seen by TG and hot-stage microscopy. At the same time, transition from crystal form A into mod. II takes place. Thus, the second endothermic peak at 157°C (onset temperature) corresponds to the melting peak of mod. II. The distinct mass loss of form A between 110 and 130°C varies between 1.9 and 4.2% depending on crystallization conditions, pre-treatment and preceded storage. A further weight loss is recorded by TG from 160°C due to volatile decomposition products, which is also perceptible in the TG-curve of mod. I or II, starting during the melting process (Fig. 3).

The water content of different samples of ground form A stored at 0% RH was determined by Karl–Fischer-titration and lies between 1.3 and 1.5%. The remaining part of the solvent corresponds to ethanol, which was proven by enzymatic analysis. Using different experimental conditions (reduced pressure, elevated temperatures and 0% RH), removal of all of the solvent from crystal form A without destroying its crystal structure was attempted. A totally solvent-free form A representing an isomorphic desolvate [13] could not be manifested.

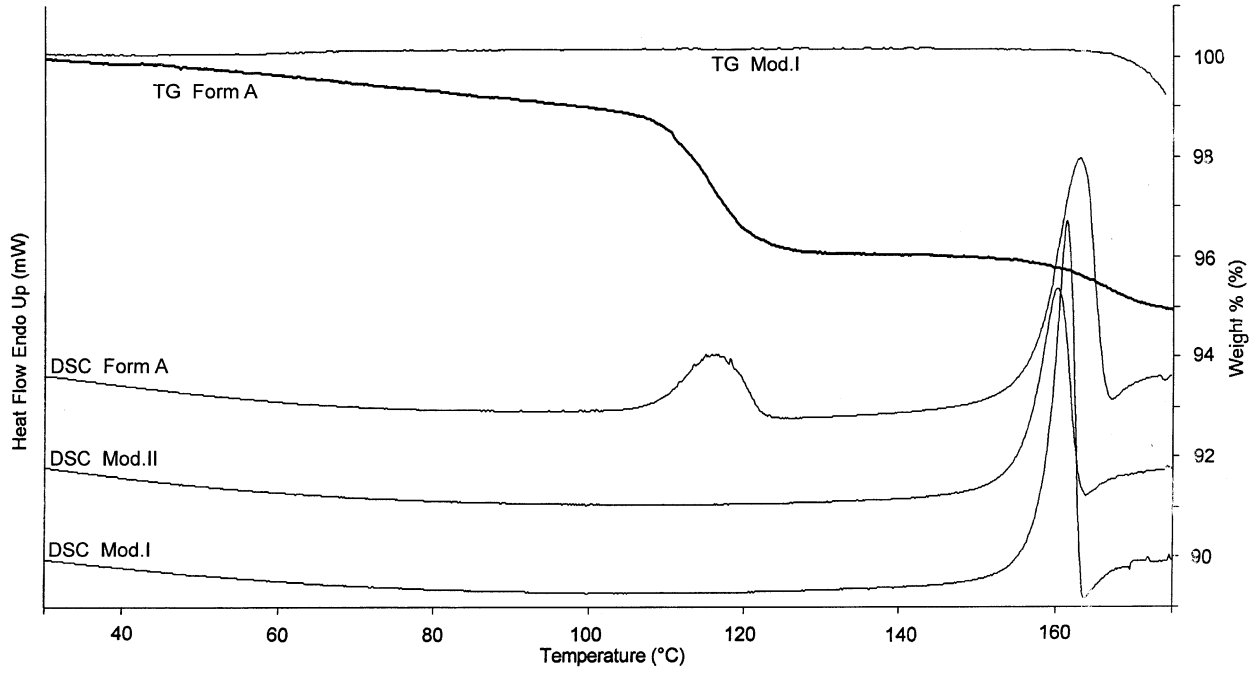

Fig. 3. DSC-curves of mod. I, mod. II, and form A (heating rate, 5 K min^{-1}, perforated pan); TG-curves of mod. I and form A (heating rate, 5 K min^{-1}).

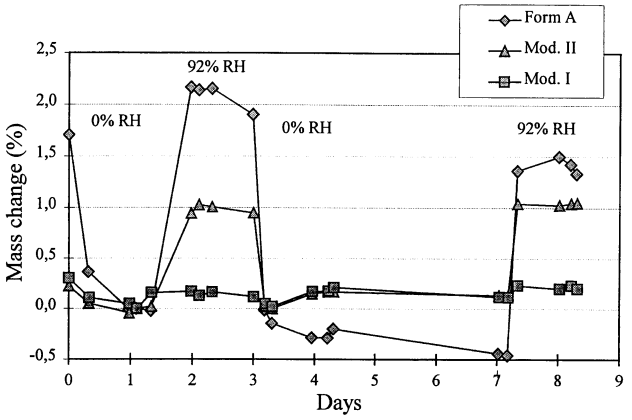

Fig. 4. Water sorption (92% RH) and desorption (0% RH) of mod. I, II, and form A at 25°C.

After 1 day of storage of the ground crystal forms at 0% RH, water sorption and desorption were determined (Fig. 4). The hygroscopicity of the three forms differs considerably. Mod. II is with 1.2% water sorption at 92% RH distinctly more hygroscopic than mod. I (0.2%), whereas ground form A exhibits the highest water uptake (2.2%). Weight loss and gain of mod. I, II and form A as a function of variation of RH are reproducible. However, the absolute weight of form A is not constant, rather it slightly decreases due to the continuous loss of included ethanol during storage in hygrostates.

FTIR- and Raman spectroscopy are useful to distinguish the three crystal forms of torasemide (Figs. 5 and 6). The most characteristic difference in the IR absorption of mod. II and form A consists of the weak absorption of the CO-band at 1697 cm^{-1}, in contrast to mod. I. This essential feature of mod. I corresponds to results obtained from single crystal data [4,5,9]. In the asymmetric unit of mod. I, there are two independent molecules with distinctly different conformations. They are linked over a very short N…N bond (2.778 Å) originated from the sulfonyl nitrogen and the pyridyl nitrogen [4]. However, the carbonyl groups are not involved and therefore enabled to fully absorb the IR at 1697 cm^{-1}. However, in the two molecules of the asymmetric unit cell of mod. II and form A, respectively, the proton of the SO_2NH group is transferred to the pyridyl group. Intermolecular hydrogen bonds between pyridyl nitrogen and sulfonyl, as well as carbonyl groups, respectively, are formed, and link the two molecules [5,9]. As a result, the hydrogen bound carbonyl groups only contribute to a weak IR absorption. The most important difference between the IR-spectra of mod. I and II in comparison with form A concerns the fusion of the first two bands in the spectrum of form A. Apart from that, the FTIR-spectra of mod. II and form A resemble each other. Distinct differences in the Raman-spectra of these two crystal forms are found in the range of aromatic and aliphatic C—H stretching bands between 3100 and 2900 cm^{-1}. The non-identical lattice vibration (especially at about 250 cm^{-1}) indicates a non-isomorphous relationship between form A and mod. II. FTIR- and Raman spectra of differently solvated crystals of form A are almost identical, regardless of whether form A was crystallized from mixtures of water with methanol, ethanol, 1- or 2-propanol.

The X-ray powder patterns of mod. I, II and form A are

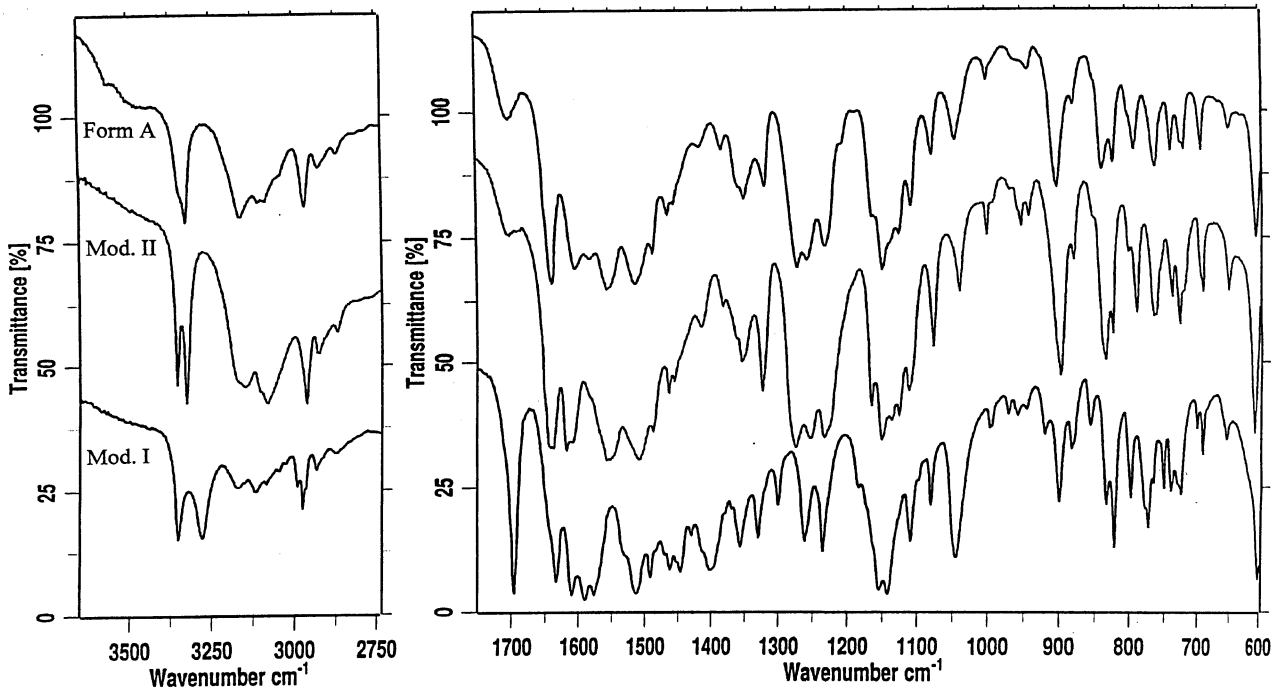

Fig. 5. FTIR-spectra of mod. I, mod. II, and form A (potassium bromide method).

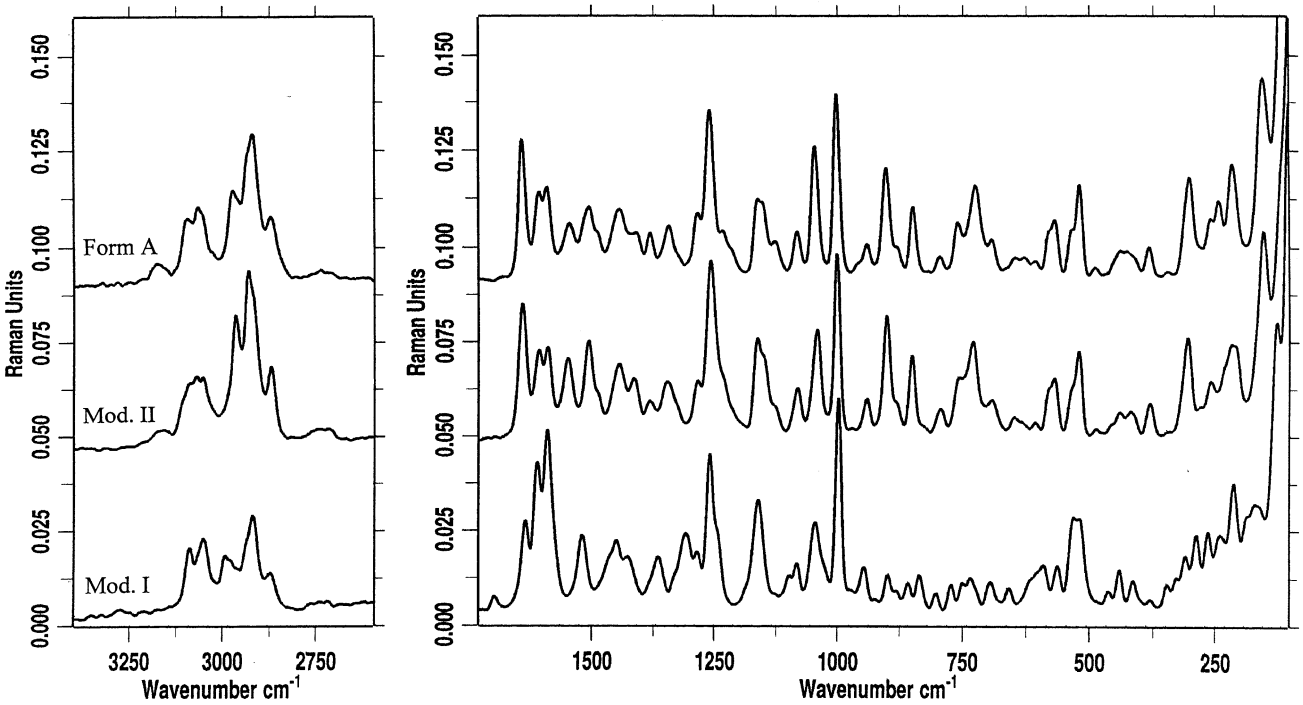

Fig. 6. Raman spectra of mod. I, mod. II, and form A.

depicted in Fig. 7. In addition, the powder pattern of form A recorded by humidity controlled diffractometry at 0% RH (after 24 h) is shown for comparison with the pattern recorded at ambient conditions. Slight shifts and distinctive intensity changes are detectable.

Powder patterns were calculated from single crystal structure data [4,5,9,14] as recommended by Bar and Bernstein [15]. In Fig. 8, the computed diffractograms are compared with measured powder patterns of mod. I, II and form A. In this way, the identity of mod. I with *Dupont's form I* was confirmed, but the identity of mod. II with *Dupont's form II* can be disclosed. However, X-ray

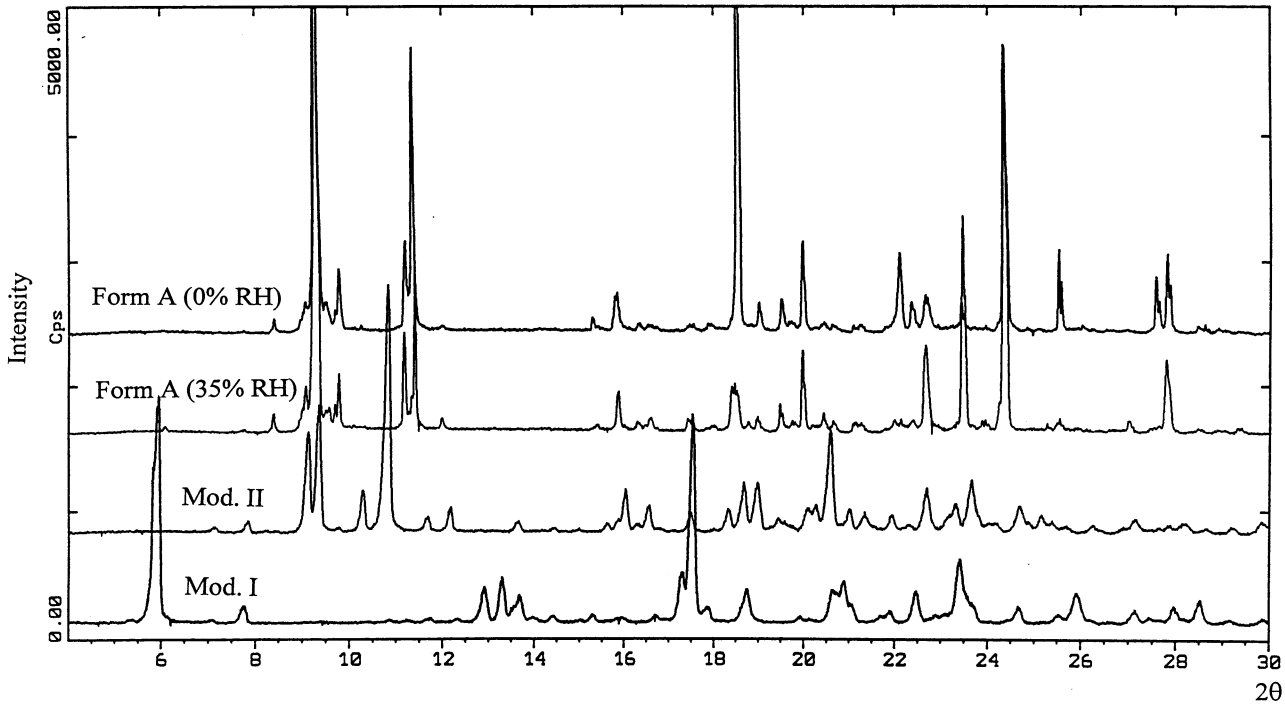

Fig. 7. X-ray powder pattern of mod. I, II, form A at ambient conditions (35% RH) and form A at 0% RH.

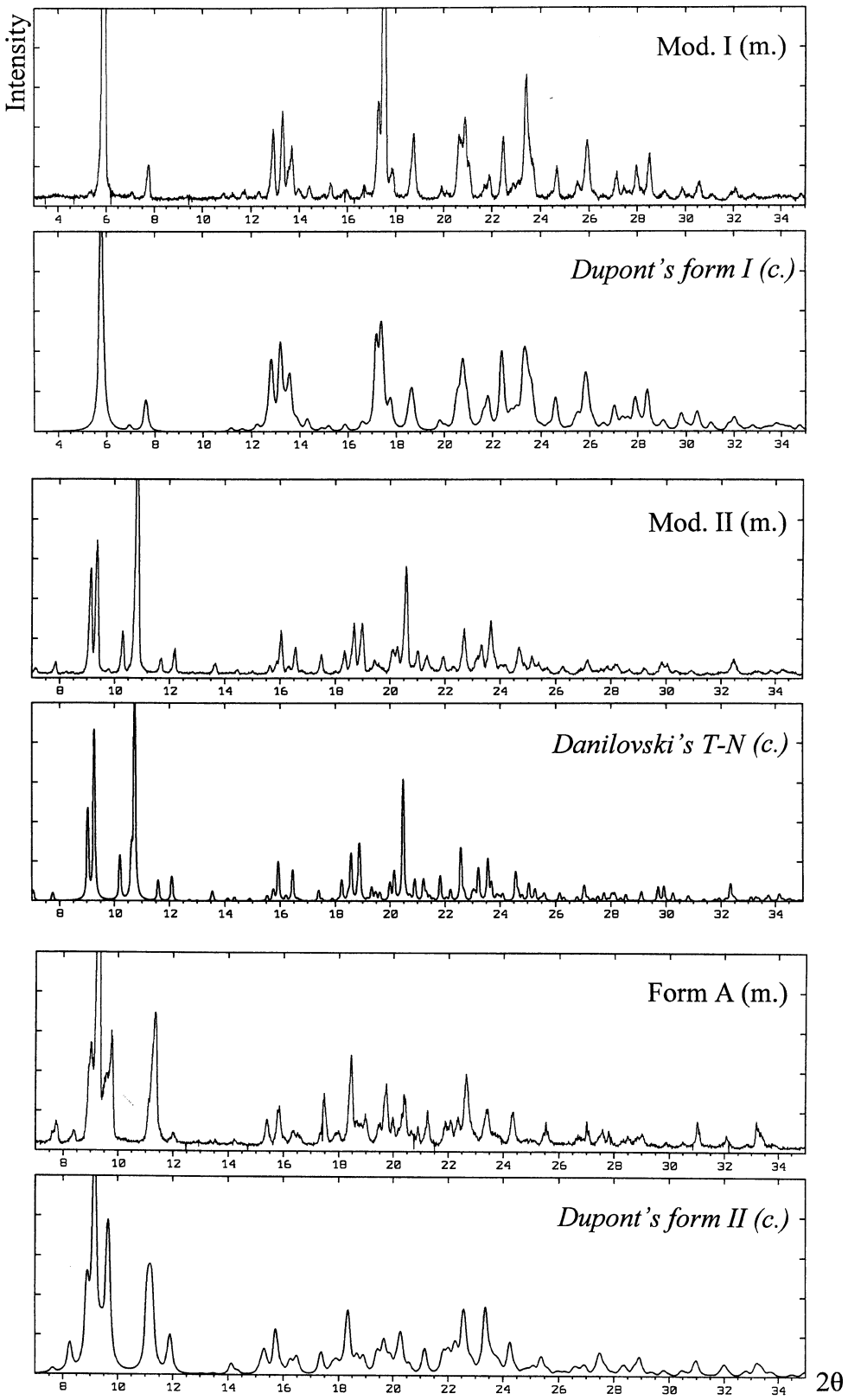

Fig. 8. Calculated (c.) diffractograms from single crystal data (Dupont's form I, II, and Danilovski's T-N), compared with measured (m.) powder patterns of mod. I, II, and form A.

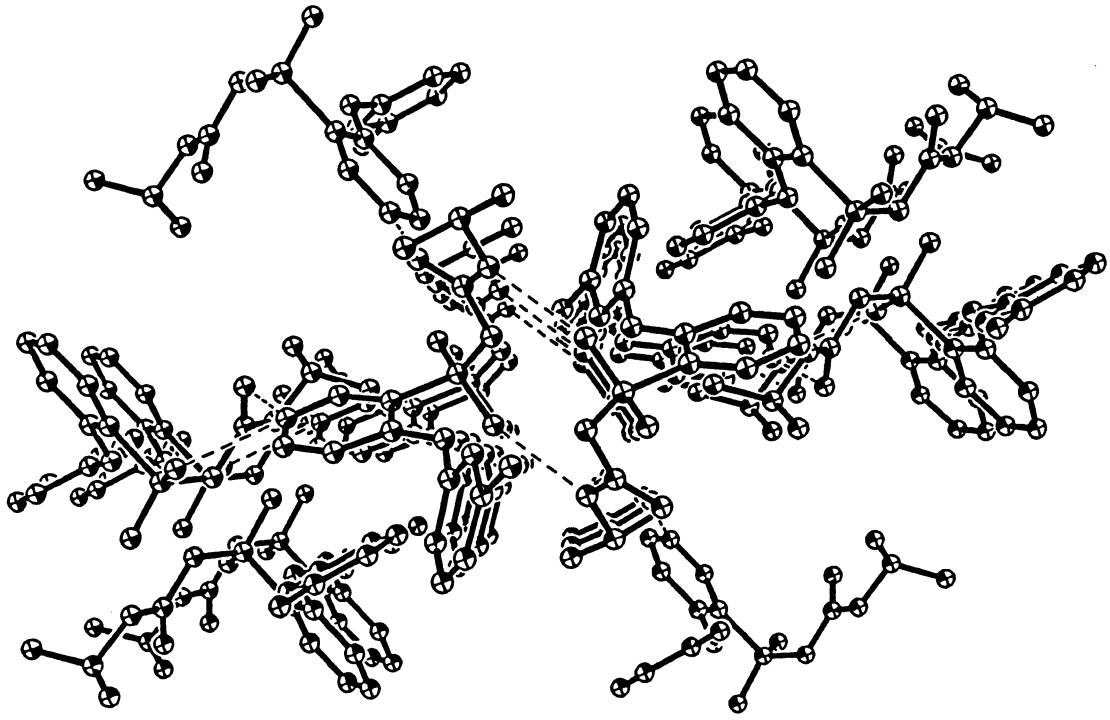

Fig. 9. Molecular arrangement of torasemide crystal form A, perspective in direction of the *b*-axis.

diffraction identity is given between single crystal structure of *Dupont's form II* and crystal form A, as well as between the crystal structure of *Danilovski's T-N* and mod. II.

Single crystal structure data of *Dupont's form II*were used to visualize the molecular arrangement of crystal form A. In Fig. 9, the existence of continuous tunnels of different sizes with a diameter of about 3–10 Å can be seen parallel to the *b*-axis of the unit cell. Probably, due to a disorder of the solvent molecules, their presence may have been overlooked in the X-ray single crystal diffraction study [5].

The measured true densities of mod. I, II and ground crystal form A (crystallized from ethanol 96%/water, v/v = 2:1) were determined and are given in Table 1. The density of mod. I is about 4.7% higher than that of mod. II and 6.1% higher than that of form A. The relative density difference between mod. II and crystal form A comes to 1.3%.

3.3. Relative stability

In order to determine the relative stability of mod. II, it was suspended in various solvents and stirred at room temperature. In fixed time intervals, suspended crystals were filtered off and their solid phase was subsequently determined by FTIR-spectroscopy. In Table 2, the time intervals within which no transition in mod. I could be detected, as well as those time intervals within which the transition in mod. I was finished, are given for different solvents.

Transition behaviour of form A was investigated by stirring a suspension in water in the same way as described above. Transition in mod. I did not occur within the first hour and was completed after 3 h. No transition in mod. II was detected. By storage of form A at ambient conditions, its crystal structure was maintained over 2 years. However, at 92% RH and 25°C, it quantitatively transformed into mod. I within 6 weeks. Form A also transformed into mod. I at 0% RH and 25°C within 8 weeks.

3.4. Dissolution behaviour

Solubility experiments were carried out with the practically relevant mod. I and II.

The saturation solubility $C_s(T)$ dependent on the tempera-

Table 2
Determination of relative stability of mod. II by stirring of suspensions with magnetic stirrer[a] and fluctuating temperatures between 15 and 20°C every 90 min

Solvent	Transformation into mod. I	
	Not before (h)	At the latest (h)
Methanol	2	3
Ethanol 96%	3	6
1-Butanol	3	24
1-Propanol	6	24
Acetone	29	49
2-Propanol	72	96
Water	96	144
1-Heptane	480	–

[a] At 900 revs./min.

Table 3
Solubility, C_s[a], in 1-butanol measured and calculated with Eq. (1), as well as its difference, and the difference[b] of solubility, ΔQ, between mod. I and mod. II[c]

Temperature (°C)	Mod. I			Mod. II			ΔQ
	$C_{s,m}$	$C_{s,c}$	Difference (%)	$C_{s,m}$	$C_{s,c}$	Difference (%)	
4.3	1.11	1.12	−1.0	3.56	3.59	−0.9	3.21
12.0	1.61	1.56	3.3	4.97	4.82	3.0	3.09
20.0	2.20	2.29	−4.1	6.42	6.67	−3.8	2.91
29.0	3.80	3.69	3.0	10.08	9.80	2.9	2.65
38.0	6.09	6.18	−1.4	14.44	14.65	−1.4	2.37
47.0	10.7	10.70	0.4	22.3	22.2	0.4	2.08

[a] Measured in mmol l^{-1}.
[b] Ratio.
[c] M, measured; C, calculated.

ture, T (in Kelvin), of mod. I and II of torasemide was determined in 1-butanol. As shown earlier (for example, in [16–18]), the general Eq. (1) was fitted to the data (Table 3) by the method of least squares (regression parameters for mod I: $a_0 = -499.95$, $a_1 = 18284.59$, $a_2 = 77.18$; for mod. II: $a_0 = -294.34$, $a_1 = 9956.05$, $a_2 = 46.17$). In Table 3, the measured and calculated results are depicted. At 20°C, mod. II is nearly three times more soluble than mod. I (Fig. 10).

$$\ln C_s(T) = a_0 + a_1 T^{-1} + a_2 \ln T \quad (1)$$

The saturation solubility C_s(pH) of mod. I and mod. II of torasemide dependent on the pH was determined at 20.0 and 38.0°C. Eq. (2) was adjusted to the data by iteration.

$$C_s(\mathrm{pH}) = C_{s,0}\left(1 + 10^{\mathrm{p}K_{a,1} - \mathrm{pH}} + 10^{\mathrm{pH} - \mathrm{p}K_{a,2}}\right) \quad (2)$$

$C_{s,0}$ is equivalent to the solubility of non-dissociated molecules of a saturated solution; $pK_{a,1}$ and $pK_{a,2}$ are the dissociation constants. They are shown for 20.0 and 38.0°C in Table 4. Fig. 11 shows the results together with the calculated plots. Due to the low wettability of torasemide in water, investigations with additional polysorbate 80 were carried out in the vicinity of the isoelectrical point pK_i at 20.0°C and pH 4.97. Only small differences result in comparison with the solubility data obtained without a surface active agent (data not shown).

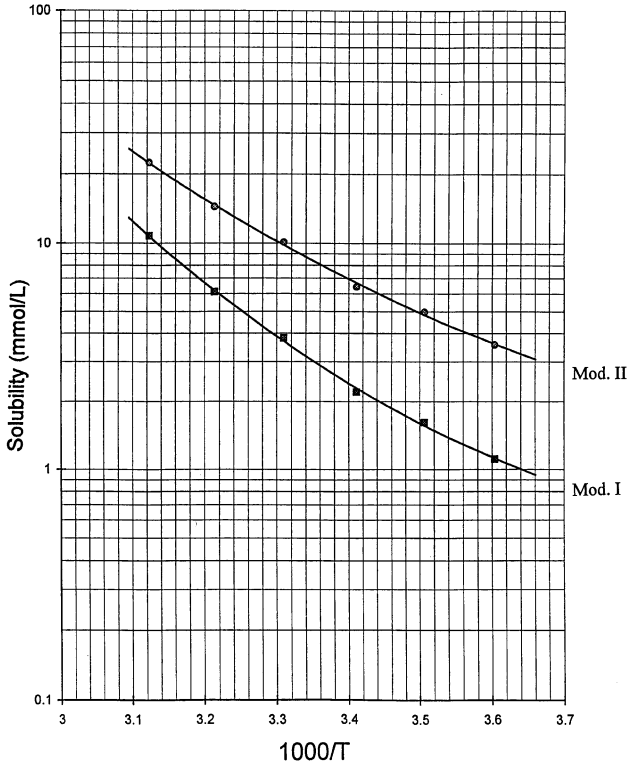

Fig. 10. Van't Hoff diagram of the solubility of mod. I and II in 1-butanol dependent on temperature (T in K, measured values and regression curves calculated on the basis of Eq. (1)).

3.5. Determination of enthalpies of solution

Enthalpies of solution (ΔH_s) of mod. I, II, and form A were measured by solution calorimetry and are given in Table 1. The difference in enthalpies of solution of mod. I and II ($\Delta H_{s,II} - \Delta H_{s,I}$) is about −4.4 kJ mol^{-1} at 40°C, whereas the difference of their enthalpies of fusion ($\Delta H_{f,II} - \Delta_{Hf,I}$) comes to about −8.2 kJ mol^{-1} (at about 160°C, determined by DSC; Table 1). These energetic differences allow an estimation of the enthalpy of transition of mod. II into I. of between 40 and 160°C (see Table 1).

Table 4
Dissociation constants[a] and basal solubility[b]

Temperature	20.0°C	38.0°C
$pK_{a,1}$	2.73	2.60
$pK_{a,2}$	7.06	6.69
pK_i (isoelectrical point)	4.90	4.65
$C_{s,0}$, mod. I (mmol l^{-1})	0.34	0.58
$C_{s,0}$, mod. II (mmol l^{-1})	0.92	1.27

[a] $pK_{a,1}$ and $pK_{a,2}$.
[b] $C_{s,0}$.

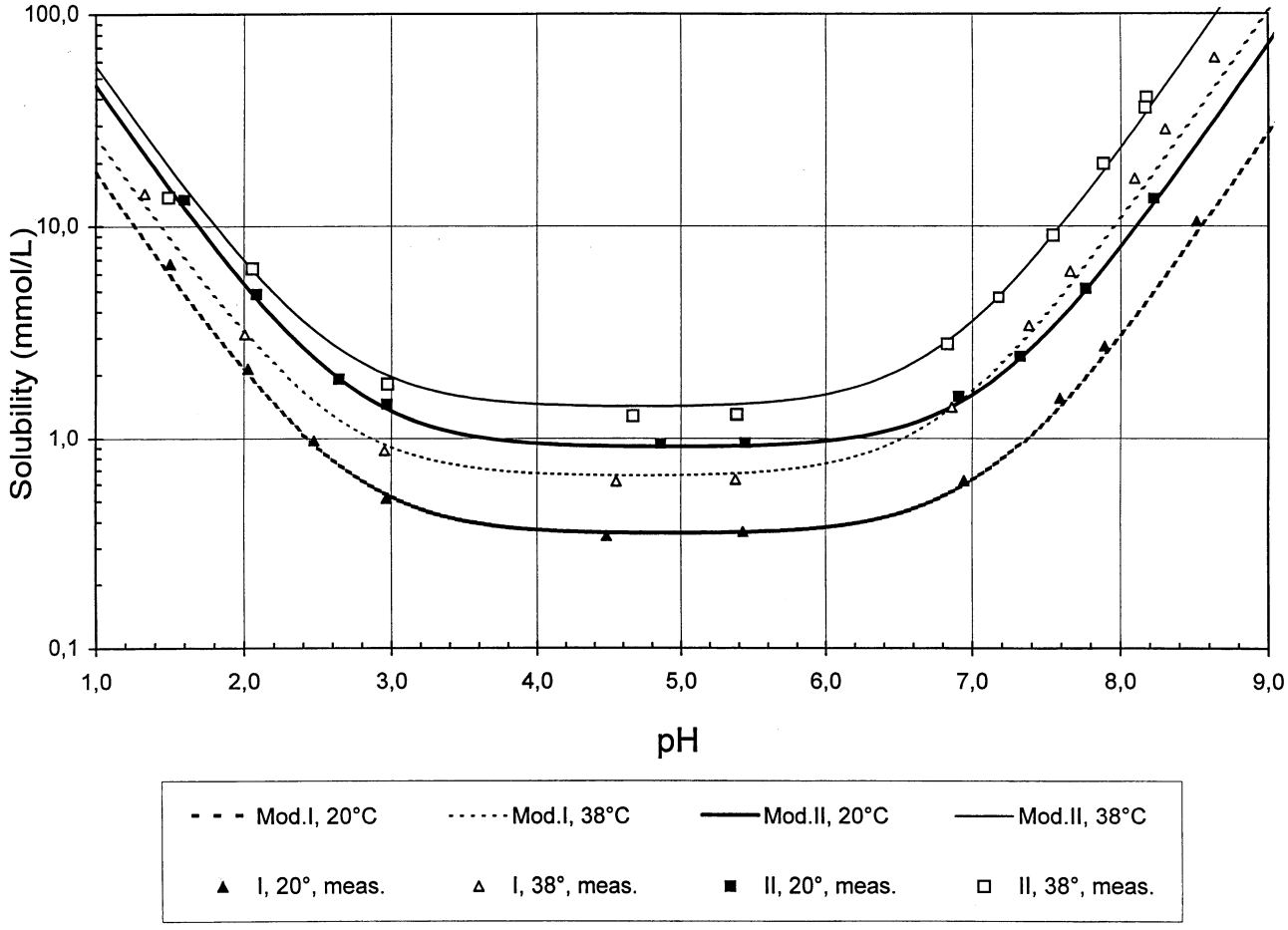

Fig. 11. Solubility of torasemide mod. I and II as function of pH at 20.0 and 38.0°C.

4. Discussion

Thermodynamic data and application of heat-of-fusion rule and density rule [19,20] revealed a monotropic relationship between mod. I and II. Stability tests, dissolution behaviour, heats of solution and investigation of hygroscopicity confirmed these results: so the higher melting mod. I is the thermodynamically stable modification over the entire temperature range. However, mod. II has a high kinetic stability, as demonstrated by thermal analysis and stability tests, and is nearly three times more soluble in water at 20°C than mod. I. Since torasemide is well bioavailable [2], a significant improvement is not to be expected by usage of the better soluble, but thermodynamically unstable mod. II.

Melting point discrepancies from the literature are due to a slight decomposition of torasemide during the melting process. According to the respective method used for determination of the melting points, and various factors such as HR and particle size [21], the values differ considerably. In addition, the melting point difference between mod. I and II is rather small, so that the identification of mod. I and II is very difficult by means of their melting points. Analytical tools of choice are IR- and Raman-spectroscopy, as well as X-ray powder diffractometry, as demonstrated in Figs. 5–7.

The results of our investigations clearly indicated that the two crystal structures published in 1978 [4,5] are representing mod. I (monoclinic, $P2_1/c$, *Dupont's form I*) and form A (monoclinic, P2/n, *Dupont's form II*). Since crystal form A is an inclusion compound, and therefore a pseudopolymorphic crystal form by definition, the term modification is incorrect. In the subsequent literature [6–8], an erroneous assignment of *Dupont's form II* (i.e. form A) to mod. II is observed. This is based on the fact that Dupont et al. [4,5] characterized their *form II* (monoclinic, P2/n, i. e. form A) with the melting point of mod. II (monoclinic, $P2_1/c$, *Danilovski's T-N*). During heating of crystal form A, it desolvates and transforms into mod. II. This process, as shown in Fig. 2a,b, was not realized, and therefore the authors did not differentiate between form A and mod. II.

By twisting the molecular arrangement of the torasemide packing of crystal form A, it is evident that crystal form A forms a framework built of hydrogen bonds and having cavities in the form of continuous channels of different sizes parallel to the *b*-axis (Fig. 9). The relatively large channels allow easy passage of solvent molecules (i.e. water plus alcohol with 1–3 C-atoms) down to about 1.9% solvent content without disruption to the packing arrangements. Crystal form A is not very stable under extreme RH condi-

tions (i.e. 0 and 92% RH), and therefore is without practical relevance in the preformulation. However, form A is of high analytical interest, because its tendency to crystallize or co-crystallize from frequently used organic solvents (i.e. methanol/water, ethanol and propanol) is very high.

Acknowledgements

The authors thank Roche Diagnostics GmbH, Germany, for supplying torasemide mod. I and II.

References

[1] A. Burger, J.M. Rollinger, Neue Erkenntnisse über Polymorphie und Pseudopolymorphie von Torasemid, Sci. Pharm. 66 (1998) S23.
[2] T. Bölke, T. Achhammer, Torasemide: review of its pharmacology and therapeutic use, Drugs Today 30 (1994) 1–26.
[3] D.C. Brater, Benefits and risks of torasemide in congestive heart failure and essential hypertension, Drug Saf. 14 (1996) 104–120.
[4] L. Dupont, J. Lamotte, H. Campsteyn, M. Vermeire, Structure cristalline et moleculaire d'un diurétique dérivé de l'alkyl-1[(phénylamino-4 pyridyl-3)sulfonyl]-3 urée: la torasemide ($C_{15}H_{20}N_4SO_3$), Acta Cryst. B 34 (1978) 1304–1310.
[5] L. Dupont, H. Campsteyn, J. Lamotte, M. Vermeire, Structure d'une seconde variété de la torasemide, Acta Cryst. B 34 (1978) 2659–2662.
[6] F. Topfmeier, G. Lettenbauer, Verfahren zur Herstellung einer stabilen Modifikation von Torasemid sowie Arzneimittel enthaltend Torasemid, EP 0 212 537 B, 1986.
[7] F. Topfmeier, G. Lettenbauer, Pharmaceutical composition containing a stable modification of torasemide, US Patent Ref. 34,672, 1994.
[8] N. Kondo, M. Kimura, M. Yamamoto, H. Hashimoto, K.-I. Kawamata, K. Kawano, H. Schmidt, Chemical structure and physico-chemical properties of torasemide, Iyakuhin Kenkyu 25 (1994) 734–750.
[9] A. Danilovski, D. Filić, M. Orešić, M. Dumić, Chemistry of torasemide. Molecular and crystal structure of new polymorph N [Crystallographic data obtained from the Cambridge Crystallographic Data Centre (CCDC, Cambridge, UK)], Croat. Chem. Acta 74 (2001) 103–120.
[10] W. Kraus, G. Nolze, PowderCell for Windows (V 1.0): Program for Manipulation of Crystal Structures and Calculation of X-ray Powder Patterns, Berlin, Germany, 1997.
[11] I. Wadsö, Calculation methods in reaction calorimetry, Sci. Tools 13 (1966) 33–39.
[12] U.J. Griesser, A. Burger, The effect of water vapor pressure on desolvating kinetics of caffeine 4/5-hydrate, Int. J. Pharm. 120 (1995) 83–93.
[13] G.A. Stephenson, E.D. Groleau, R.L. Kleemann, W. Xu, D.R. Rigsbee, Formation of isomorphic desolvates: creating a molecular vacuum, J. Pharm. Sci. 87 (1998) 536–542.
[14] L. Dupont, G. Dive, Torasemide: a comparison of two refinement computer programs and effects on CNDO/2 calculations, Bull. Soc. Sci. Liège 51 (1982) 248–255.
[15] I. Bar, J. Bernstein, Conformational polymorphism VI: the crystal and molecular structures of form II, III and V of 4-amino-*N*-2-pyridinylbenzenesulfonamide (sulfapyridine), J. Pharm. Sci. 74 (1985) 255–263.
[16] A. Burger, Löslichkeitsuntersuchungen zur Ermittlung thermodynamischer Daten eines polymorphen Arzneimittels (Sulfanilamid), Sci. Pharm. 41 (1973) 303–314.
[17] A. Burger, Dissolution and polymorphism of metolazone, Arzneimittelforschung 25 (1975) 24–27.
[18] A. Burger, U.J. Grießer, The polymorphic drug substances of the European Pharmacopoeia. Part 7: Physical stability, hygroscopicity and solubility of succinylsulfathiazole crystal forms, Eur. J. Pharm. Biopharm. 37 (1991) 118–124.
[19] A. Burger, Zur Interpretation von Polymorphieuntersuchungen, Acta Pharm. Technol. 28 (1982) 1–20.
[20] A. Burger, R. Ramberger, On the polymorphism of pharmaceuticals and other molecular crystals. II: Applicability of thermodynamic rules, Mikrochim. Acta 1979II (1979) 273–316.
[21] M. Kuhnert-Brandstätter, Thermomicroscopy of organic compounds, in: G. Svehla (Ed.), Wilson and Wilson's Comprehensive Analytical Chemistry, Vol. XVI, Elsevier, Amsterdam, 1982, pp. 351–353.